

Structural properties and thermodynamic stability of Ba-doped silicon type-I clathrates synthesized under high pressure

Akiko Kitano,* Koji Moriguchi,[†] Mitsuharu Yonemura, Shinji Munetoh, and Akira Shintani[‡]
Electronics Engineering Laboratories, Sumitomo Metal Industries, Ltd., 1-8 Fusochō, Amagasaki, Hyogo 660-0891, Japan

Hiroshi Fukuoka and Shoji Yamanaka
Department of Applied Chemistry, Faculty of Engineering, Hiroshima University, 1-4-1 Kagamiyama, Higashi-Hiroshima, Hiroshima 739-8527, Japan

Eiji Nishibori, Masaki Takata, and Makoto Sakata
Department of Applied Physics, Nagoya University, Nagoya 464-8603, Japan
 (Received 31 August 2000; revised manuscript received 6 February 2001; published 29 June 2001)

We present a joint experimental and theoretical study of the stability and structural properties of Ba-doped silicon type-I clathrates $\text{Ba}_8\text{Si}_{46}$ synthesized under high pressures. The thermodynamic stability of $\text{Ba}_8\text{Si}_{46}$ under high pressure has been discussed from the total energy calculations of some barium silicides within the local density approximation (LDA). We have theoretically found that pressure favors the formation of the clathrate phase as experimentally observed. We have also performed a synchrotron x-ray-diffraction experiment of $\text{Ba}_8\text{Si}_{46}$ prepared under high pressures. Some of the missing endohedral Ba elements in the small cage of Si(20) have been observed by x-ray crystallography, while big cages of Si(24) are found to be completely occupied by Ba elements. The stabilization energies of Ba atoms in the endohedral sites estimated within the present LDA calculation suggest that this is presumably attributed to the energetical site preference of Ba atoms between $d(6)$ and $a(2)$ sites. In addition, the isothermal parameter of Ba in the big cage of Si(24) has been found to be larger than that in the small Si(20) unit, which is consistent with some theoretical predictions in earlier works.

DOI: 10.1103/PhysRevB.64.045206

PACS number(s): 61.72.Dd, 61.48.+c

I. INTRODUCTION

Expanded-volume silicons and/or germaniums, called clathrates, have drawn considerable interest over the past few years. Clathrates are covalent-cage-like assembled crystals analogous to fullerene families.^{1–3} These structures form large polyhedral cavities that can accommodate guest elements allowing a wide variety of novel compounds. Though two forms of clathrates such as Si_{46} (type I) and Si_{34} (often referred to as Si_{136} , type II) have been known for many years,^{1,2} two experimental phenomena recently confirmed in clathrates have triggered intensive investigation. One is the discovery of superconductivity in the metal-doped clathrate $\text{Ba}_x\text{Na}_y\text{Si}_{46}$,^{4–7} and the other is the potential of clathrates for thermoelectric applications, where the figure of merit can be made arbitrarily large with the “phonon glass and electron crystal (PGEC)” mechanism.^{8–10} Clathrate structures are also considered as potential candidates for the band gap engineering based on group-IV elements. This is because the guest-free clathrate structures such as Si_{34} , Si_{46} , Ge_{34} , and Ge_{46} have been theoretically predicted to have a much larger band gap than their ground state of cubic diamond phase.^{11–21} Recently, these theoretical predictions have been experimentally borne out by Gryko *et al.*²²

It has been shown that some metal-doped clathrate compounds could be synthesized in a controllable manner, resulting in a desired crystal structure and a chemical composition. For example, Yamanaka *et al.*⁷ have utilized high pressures to succeed in the synthesis of “bulk” barium-doped binary

silicon clathrate compounds $\text{Ba}_8\text{Si}_{46}$ instead of “powder” compounds. The researchers involved have also observed type-II superconductivity with the critical temperature (T_c) of approximately 8 K in this silicon clathrate compound.⁷ In addition, in order to clarify a cause of the superconductive property in these Ba-doped silicon clathrates, we have also reported the electronic structure of $\text{Ba}_8\text{Si}_{46}$ and $\text{Na}_8\text{Si}_{46}$ using the first-principles calculation.²⁰ Though the conventional x-ray-diffraction and the Rietveld refinement of $\text{Ba}_8\text{Si}_{46}$ synthesized under high pressures were presented in our previous work,⁷ the microstructural properties such as occupations and/or accurate isotropic thermal parameters of the endohedral Ba atoms in this clathrate compound have not been reported. This is because our previous experiment had a comparatively large signal/noise (S/N) ratio due to using the conventional x-ray-diffraction powder method. The thermal parameters, or atomic displacement parameters (ADP’s), of endohedral atoms are important aspects of clathrate compounds, when considering the PGEC mechanism for thermodynamic applications.^{8–10}

In this work, we present a joint experimental and theoretical study of the stability and structural properties of Ba-doped silicon type-I clathrates $\text{Ba}_8\text{Si}_{46}$ synthesized under high pressures. We have carried out total energy calculations of some barium silicides within the local density approximation (LDA), and discussed why the Ba-doped Si clathrate $\text{Ba}_8\text{Si}_{46}$ can be synthesized utilizing high pressures. In addition, we have performed a synchrotron x-ray-diffraction experiment of the $\text{Ba}_8\text{Si}_{46}$ prepared under high pressures, using

the BL02B2 powder-diffraction beam line at SPring8 (Hyogo, Japan). We will report occupations and isotropic thermal parameters of the endohedral Ba atoms in this clathrate compound. We have found some of the missing endohedral Ba elements in the small cage of Si(20). The isothermal parameter of Ba in the big cage of Si(24) has been found to be larger than that in the small Si(20) unit, which is consistent with some theoretical predictions in earlier works.^{23–26}

II. METHODOLOGY

A. Theoretical

The main purpose of the present theoretical calculations is to examine equations of state of some barium silicides in order to discuss the thermodynamic stability of the clathrate phase under high pressures. We have calculated total energies versus volume for bcc-Ba, cd-Si (cubic diamond Si), BaSi, BaSi₂, Si₄₆, and Ba₈Si₄₆. Since a nonstoichiometric compound of Ba_{8-x}Si₄₆ has been experimentally prepared utilizing high pressures as will be described later, we have also calculated energetics and electronic states of Ba₂Si₄₆ and Ba₆Si₄₆, in which endohedral Ba atoms at *d*(6) or *a*(2) sites have been excluded from Ba₈Si₄₆. BaSi₂ is known to have three crystallographic forms at ambient conditions orthorhombic, cubic, and trigonal.²⁷ The orthorhombic BaSi₂ is stable at ambient conditions, and the others are metastable.²⁷ We have experimentally found that the arc-melted prepressured sample is a mixture of the orthorhombic BaSi₂ and cd-Si,⁷ therefore, the orthorhombic BaSi₂ has been adopted for the present calculation.

Our calculations are based on the *ab initio* pseudopotential theory within the LDA. We adopted the ultrasoft pseudopotential proposed by Vanderbilt.²⁸ The Perdew-Zunger parametrization²⁹ of the LDA was employed. We used the CASTEP code³⁰ in order to self-consistently solve the pseudopotential Schrödinger equation. From the convergence tests of total energies, we chose the kinetic energy cutoff of 300 eV of plane-wave basis sets for all systems studied. For the Brillouin zone sampling, we adopted 84, 28, 27, 24, 10, and 20 special *k* points for bcc-Ba, cd-Si, BaSi, BaSi₂, Si₄₆, and Ba-doped type-I clathrates (Ba₂Si₄₆, Ba₆Si₄₆, and Ba₈Si₄₆), respectively. Optimized geometry and electronic structure of Ba₈Si₄₆ have already been reported in our previous work (see also in Table II).²⁰ The bulk moduli were deduced by applying a fitting procedure of the total energies versus volume to the Murnaghan's equation of state.

B. Experimental

The bulk samples of Ba₈Si₄₆ crystal were synthesized by a method utilizing high pressures reported in the previous work.⁷ The present sample was synthesized with the pressure applied by 3 GPa at 800 °C. Powder samples of Ba₈Si₄₆ for x-ray-diffraction experiments were prepared by the precipitation method and a fine powder was sealed in 0.3 mm ϕ silica glass capillary. The x-ray-powder-diffraction data was measured by the synchrotron radiation powder method using the large Debye Scherrer Camera with Imaging Plate at BL02B2 in SPring8.³¹ The wavelength of the incident x ray

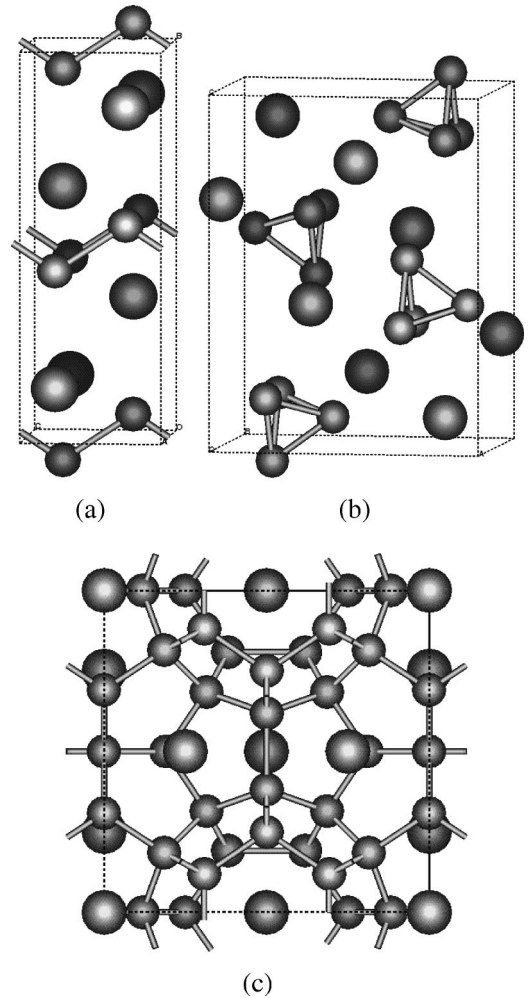


FIG. 1. Schematic illustrations of crystal structures of (a) BaSi, (b) BaSi₂, and (c) Ba₈Si₄₆. Endohedral Ba atoms at *d*(6) and *a*(2) sites have been excluded from Ba₈Si₄₆ for Ba₂Si₄₆ and Ba₆Si₄₆, respectively (see also Table II).

is 0.4979 Å. In order to correct data with high counting statistics, the exposure time was 25 min. The crystal structure was refined by the Rietveld method, which was carried out using the computer program RIETAN97 β .³² The initial crystal model for the Rietveld refinement was referred to the model in our previous work.⁷

III. RESULTS AND DISCUSSION

A. Theoretical energetics

We show schematic illustrations of crystal structures of barium silicides calculated in the present work in Fig. 1. The resulting equilibrium structures and inequivalent atomic positions are listed in Tables I and II. Though all of the lattice constants calculated here are slightly shorter than those of the experimental values, which is the well-known property using the LDA approximation,^{33–35} the calculated atomic positions for BaSi, BaSi₂, and Ba₈Si₄₆ agree well with the experimental positions.^{7,36,37} In addition, the calculated lattice constant ratios *a*:*b*:*c*, for BaSi and BaSi₂ are 1: 2.38: 0.81

TABLE I. Calculated equilibrium structures and inequivalent atomic positions for bcc-Ba, cd-Si, BaSi, and BaSi₂. The notation of atomic positions follows that of the International Tables for Crystallography. Experimental values of barium silicides (BaSi and BaSi₂) are also listed.

	bcc-Ba	cd-Si
Symmetry	$Im\bar{3}m$ (229)	$Fd\bar{3}m$ (227)
Lattice constant (Å)	4.758	5.381
	Ba: $a(2)$ $x,y,z=0$	Si: $a(8)$ $x,y,z=0$
	BaSi	Exp.: BaSi ^a
Symmetry	$Cmcm$ (63)	$Cmcm$ (63)
Lattice constant (Å)	$a=4.951$, $b=11.787$, $c=4.019$	$a=5.043$, $b=11.933$, $c=4.1395$
Si: $c(4)$	$x=0$; $y=0.858$; $z=3/4$	$x=0$; $y=0.8598$; $z=3/4$
Ba: $c(4)$	$x=0$; $y=0.558$; $z=3/4$	$x=0$; $y=0.5589$; $z=3/4$
	BaSi ₂	Exp.: BaSi ₂ ^b
Symmetry	$Pnma$ (62)	$Pnma$ (62)
Lattice constant (Å)	$a=8.710$, $b=6.585$, $c=11.240$	$a=8.920$, $b=6.750$, $c=11.570$
Si: $c(4)$	$x=0.420$; $y=1/4$; $z=0.092$	$x=0.424$; $y=1/4$; $z=0.091$
Si: $c(4)$	$x=0.197$; $y=1/4$; $z=0.965$	$x=0.205$; $y=1/4$; $z=0.969$
Si: $d(8)$	$x=0.195$; $y=0.070$; $z=0.148$	$x=0.190$; $y=0.078$; $z=0.147$
Ba: $c(4)$	$x=0.016$; $y=1/4$; $z=0.691$	$x=0.014$; $y=1/4$; $z=0.694$
Ba: $c(4)$	$x=0.841$; $y=1/4$; $z=0.094$	$x=0.893$; $y=1/4$; $z=0.095$

^aReference 36.

^bReference 37.

and 1: 0.76: 1.29, which can be compared with the experimental values of 1: 2.37 : 0.82 for BaSi and 1: 0.76: 1.30 for BaSi₂, respectively.^{36,37}

Calculated lattice constants of Ba-doped type-I clathrates have been slightly increased with the contents of endohedral Ba atoms as shown in Table II. It has been found, however, that the elongation of lattice constant of Ba₈Si₄₆ is only 1.2% compared with guest-free Si₄₆. Thus, the lattice constants of these clathrate structures are assumed to be not so sensitive to the existence of endohedral metals in the cage structures. In Na-doped type-II Si clathrates, Ramachandran *et al.* have experimentally observed only a $\sim 0.5\%$ increase in the unit cell edge upon progressing from Na₄Si₁₃₆ to Na₂₃Si₁₃₆.³⁸ These results suggest that the cage size in clathrate systems strongly depend on the framework atoms,²¹ but weakly on the “guest” atoms. This property is also experimentally

pointed out in Ge clathrate compounds by Nolas *et al.*,¹⁰ in which they also suggest that appropriate “guest” atoms incorporated into the polyhedral cavities might change thermal conductivities for thermoelectric applications due to their dynamical “rattling” modes.

The stabilization energy of the endohedral Ba atoms in the Ba-doped silicon clathrate is defined as the total energy of the clathrate subtracted from the sum of the total energies of the guest-free clathrate (Si₄₆) and isolated Ba atoms. In the present work, the total energy of the isolated Ba atom is estimated using the total energy of bcc-Ba and its experimental cohesive energy. The calculated stabilization energies of the endohedral Ba atoms are 3.3, 3.8, and 3.7 eV/atom for Ba₂Si₄₆, Ba₆Si₄₆, and Ba₈Si₄₆, respectively. Therefore, Ba[$d(6)$] in the large cage of Si(24) is energetically stabler than Ba[$a(2)$] in the small unit of Si(20) by about 0.5 eV/

TABLE II. Calculated equilibrium structures and inequivalent atomic positions for clathrate phases of Si₄₆, Ba₂Si₄₆, Ba₆Si₄₆, and Ba₈Si₄₆. The notation of atomic positions follows that of the International Tables for Crystallography. Calculated values of Si₄₆ and Ba₈Si₄₆ listed here are from our previous work of Ref. 20.

	Si ₄₆ ^a	Ba ₂ Si ₄₆	Ba ₆ Si ₄₆	Ba ₈ Si ₄₆ ^a
Symmetry	$Pm\bar{3}n$ (223)	$Pm\bar{3}n$ (223)	$Pm\bar{3}n$ (223)	$Pm\bar{3}n$ (223)
Lattice constant	10.069 Å	10.106 Å	10.118 Å	10.192 Å
Si: $c(6)$	$x=1/4$; $y=0$; $z=1/2$	$x=1/4$; $y=0$; $z=1/2$	$x=1/4$; $y=0$; $z=1/2$	$x=1/4$; $y=0$; $z=1/2$
Si: $i(16)$	$x,y,z=0.184$	$x,y,z=0.185$	$x,y,z=0.184$	$x,y,z=0.185$
Si: $k(24)$	$x=0$; $y=0.308$ $z=0.117$	$x=0$; $y=0.310$ $z=0.116$	$x=0$; $y=0.305$ $z=0.120$	$x=0$; $y=0.308$ $z=0.120$
Ba: $a(2)$		$x,y,z=0$		$x,y,z=0$
Ba: $d(6)$			$x=1/4$; $y=1/2$; $z=0$	$x=1/4$; $y=1/2$; $z=0$

^aReference 20.

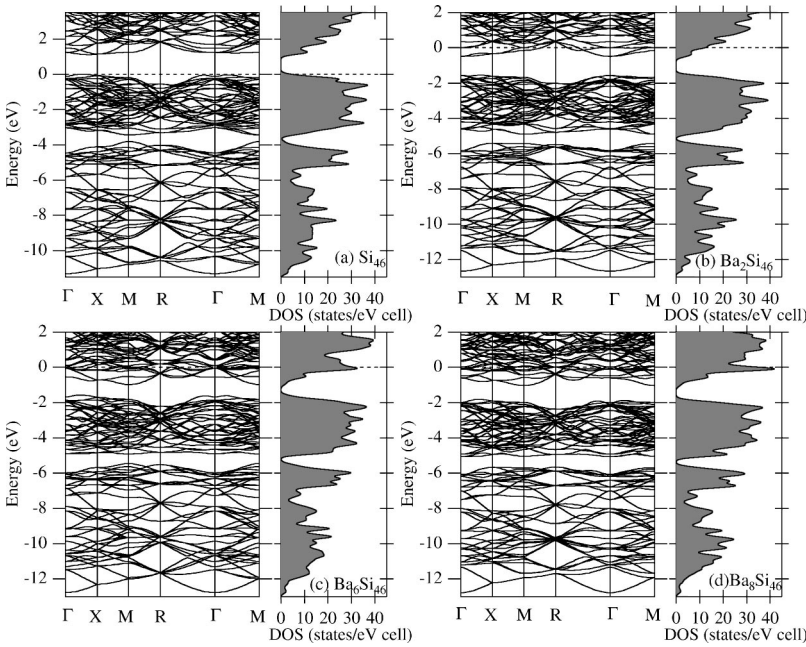


FIG. 2. Band structures and density of states for (a) Si_{46} , (b) $\text{Ba}_2\text{Si}_{46}$, (c) $\text{Ba}_6\text{Si}_{46}$, and (d) $\text{Ba}_8\text{Si}_{46}$. Density of states are calculated using 0.1 eV Gaussian broadening of the band structure. Energy is measured from the top of the valence band or the Fermi level, which is denoted by horizontal broken lines.

atom, and Ba atoms are predicted to prefer occupying the $d(6)$ sites to the $a(2)$ ones in the Si_{46} crystal structure. As will be described in the next section, some of the missing endohedral Ba elements in the small cage of Si(20) have been actually observed by x-ray crystallography. The observed missing of Ba atoms in the Si(20) unit is presumably related to this site preference of Ba atoms.

The lineup of band structures and the density of states for Si_{46} , $\text{Ba}_2\text{Si}_{46}$, $\text{Ba}_6\text{Si}_{46}$, and $\text{Ba}_8\text{Si}_{46}$ is shown in Fig. 2. Four, twelve, and sixteen valence electrons from Ba atoms in $\text{Ba}_2\text{Si}_{46}$ [Fig. 2(b)], $\text{Ba}_6\text{Si}_{46}$ [Fig. 2(c)], and $\text{Ba}_8\text{Si}_{46}$ [Fig. 2(d)] contribute to form the conduction-band edge. In the Na-doped binary clathrate of $\text{Na}_8\text{Si}_{46}$, we have reported that Na state is weakly hybridized with the Si_{46} conduction-band state and this weak hybridization results in almost rigid energy band modification of guest-free Si_{46} .²⁰ Similar theoretical results have also been presented in the K-doped type-I Ge clathrate K_8Ge_{46} , by Zhao *et al.*¹⁹ In contrast, the conduction-band dispersion of $\text{Ba}_x\text{Si}_{46}$ ($x=2, 6, \text{ and } 8$) is strongly modified from that of the guest-free Si_{46} . This is caused by the strong hybridization between the Ba states and the Si_{46} conduction-band as also suggested previously in $\text{Na}_2\text{Ba}_6\text{Si}_{46}$ by Saito and Oshiyama.¹² It is interesting to note that the density of states (DOS) at the Fermi level in $\text{Ba}_x\text{Si}_{46}$ is strongly altered with the contents of endohedral Ba atoms. The Fermi levels of $\text{Ba}_6\text{Si}_{46}$ and $\text{Ba}_8\text{Si}_{46}$ are located closely to strong peaks of DOS as shown in Figs. 2(c) and 2(d), respectively, while the DOS at the Fermi level for $\text{Ba}_2\text{Si}_{46}$ is moderate. These results suggest that hybridizations of Ba[$d(6)$] in the large cage of Si(24) with the Si_{46} conduction-band state play an important role to form a high-DOS peak at Fermi energy. These results are also reminiscent of the experimental work of Kawaji *et al.*⁶ They had prepared Ba containing ternary silicon clathrate compounds $\text{Na}_x\text{Ba}_6\text{Si}_{46}$ with various Na contents ($0.2 \leq x \leq 1.5$) by Na evaporation from $\text{Na}_2\text{Ba}_6\text{Si}_{46}$, and then reported that the critical temperature (T_c) of superconductivity increases with

the decrease of Na content in a temperature range of 4.8–2.6 K. Though the exact reason why the T_c depends on the Na content is yet uncertain, the clathrate compound with the smallest Na content $\text{Na}_{0.2}\text{Ba}_6\text{Si}_{46}$ in which $a(2)$ sites in the small cage of Si(20) are almost unoccupied, actually shows the superconductivity at $T_c=4.8$ K. We assume that the result by Kawaji *et al.* shows experimental evidence that Ba[$d(6)$] states play a crucial role for the superconductivity in Ba-doped silicon clathrates. Our present calculation results again demonstrate that the large density of states at the Fermi level $N(\epsilon_F)$ enhanced by the hybridization of Ba states with the clathrate frameworks plays a key role for the superconductivity of Ba-doped silicon clathrates as suggested in the previous works.^{12,20} Therefore, the analysis based on the conventional Bardeen-Cooper-Schrieffer (BCS) theory for phonon-mediated superconductivity is assumed to be quite effective for studying the superconductivity in silicon clathrate compounds.³⁹

We have also calculated total energies as a function of atomic volume near the equilibrium volume for each system. In these calculations for each system, we have fixed the atomic positions listed in Tables I and II. In addition, the lattice constant ratio of $a:b:c$ for BaSi and BaSi_2 has been fixed at the ratio of the equilibrium structure. In order to examine the numerical accuracy of equations of states of BaSi_2 and $\text{Ba}_8\text{Si}_{46}$ for the approximation fixing atomic positions, we have compared the energies calculated for (i) the fractional coordinates at the LDA equilibrium unit volume given in Tables I and II and (ii) the structures with the fractional coordinates optimized at a certain unit volume. These comparisons have been performed at the unit volumes compressed by 7.5% from the LDA equilibrium volumes, in which the lattice constant for $\text{Ba}_8\text{Si}_{46}$ is $a=9.918$ Å and the lattice constants for BaSi_2 are $a=8.485$ Å, $b=6.415$ Å, and $c=10.949$ Å. The total energy differences for BaSi_2 and $\text{Ba}_8\text{Si}_{46}$ within the present scheme are found to be 9.3 and 3.1 meV/atom, respectively. From the present calculations,

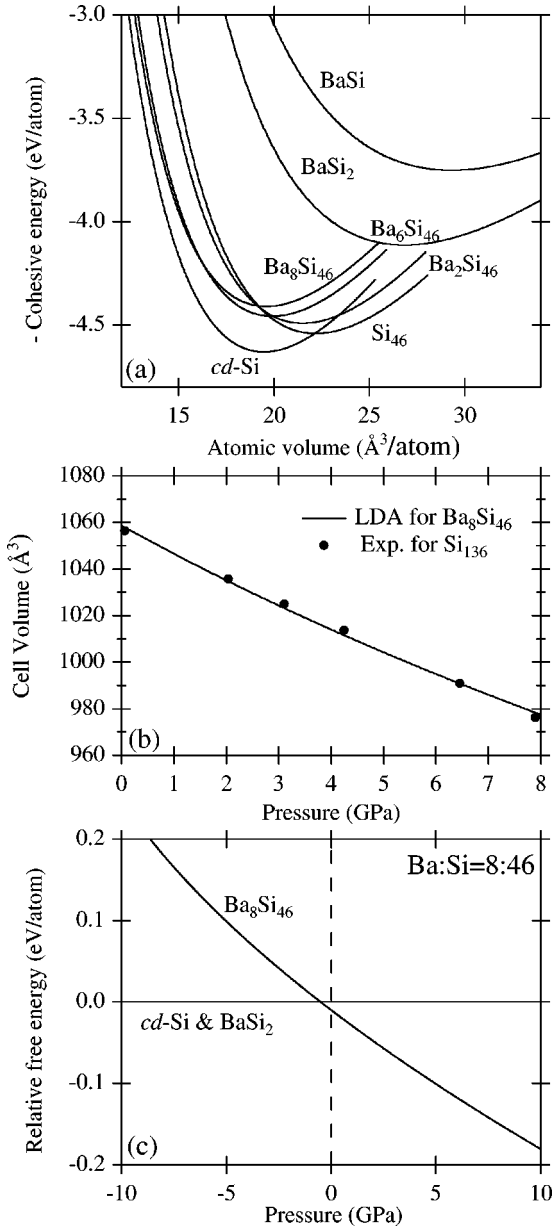


FIG. 3. (a) Equations of state of cd-Si, BaSi, BaSi₂, Si₄₆, Ba₂Si₄₆, Ba₆Si₄₆, and Ba₈Si₄₆. The calculated total energies are shifted so that the energies of bcc-Ba and cd-Si are equal to the experimental negative cohesive energies. (b) Pressure dependence of the unit volume in Ba₈Si₄₆. The experimental variation of cell volume with pressure for Si₁₃₆ from Ref. 44, which is scaled to the Si₄₆ unit volume, is also shown for comparison. (c) The relative Gibbs free energy (relative enthalpy) of Ba₈Si₄₆ to the coexisting phase of cd-Si and BaSi₂ in the case of atomic composition of Ba:Si=8:46.

the cell volume compressed by 7.5% is estimated to correspond to the equilibrium pressure of 4.8 and 7.8 GPa for BaSi₂ and Ba₈Si₄₆, respectively. Therefore, we presume that the relative enthalpy of Ba₈Si₄₆ to the coexisting phase of cd-Si and BaSi₂, which will be described later, is accurate within less than 10–20 meV/atom at about 5 GPa.

The equation of state for each system is depicted in Fig. 3(a) and the summary of calculated values are listed in Table

III. In Fig. 3(a), the calculated total energies are shifted so that the energies of bcc-Ba and cd-Si are equal to the experimental negative cohesive energies.^{40,41} Since the bulk modulus deduced using the Murnaghan’s equation of state is known to be strongly sensitive to its pressure derivative (B'), bulk moduli assuming $B' = 3.7$ of Si₄₆ are also listed in parentheses in Table III for Ba₂Si₄₆, Ba₆Si₄₆, and Ba₈Si₄₆.

The bulk moduli of type-I clathrate phases are predicted to be 83–89 GPa, which are about 9–13% smaller than that of cd-Si. The reduction of the bulk modulus for clathrates has been pointed out theoretically.^{17,18,21,42} In addition, San-Miguel *et al.*⁴³ and Ramachandran *et al.*⁴⁴ have experimentally reported bulk moduli of Si₁₃₆-based (type-II) clathrate phases along with the theoretical results. Our calculated results of clathrates are in good agreement with their experiments. The calculated bulk moduli of Ba-doped type-I clathrates were increased slightly in comparison with that of the “guest”-free silicon clathrate of Si₄₆, but not so sensitive to the existence of Ba atoms in the endohedral sites. This indicates that the hardness in clathrate systems essentially depends on the framework atoms.²¹

We show the pressure dependence of the unit volume in Ba₈Si₄₆ from LDA calculations in Fig 3(b). To the authors’ best knowledge, the experimental results of the pressure dependence of the unit volume in Si₄₆ (type I) clathrates have not yet been reported. In addition, the equation of state of guest-free Si₁₃₆ (Si₃₄) is theoretically known to be almost identical with that of Si₄₆.^{15,21,42} Therefore, the experimental variation of cell volume with pressure for Si₁₃₆ by Ramachandran *et al.*,⁴⁴ which is scaled to the Si₄₆ unit volume, is also shown in Fig 3(b) for comparison. In their experiment, the “guest”-free silicon clathrate Si₁₃₆ is used for measurements of pressure dependence of the unit volume.^{22,44} Over the pressure range from 0 to 8 GPa, Ba₈Si₄₆ is predicted to undergo ~7.5% volume change, which corresponds with the change in Si₁₃₆ experimentally observed by Ramachandran *et al.*⁴⁴ On pressurization above 8 GPa, Ramachandran *et al.* have observed the structural transition from Si₁₃₆ to β -tin phase. Similar transition has been also observed in Na_{0.6}Si₁₃₆ at a slightly higher transition pressure (11 GPa) by San-Miguel *et al.*⁴³ In contrast, transition properties of type-I clathrate compounds under high pressures have not been experimentally reported yet, as far as we know.

In order to discuss thermodynamic stability in a given chemical composition, we consider the following relative free energy:

$$\Delta G(P) = G_{\text{Ba}_8\text{Si}_{46}}(P) - \frac{(8 \times 3)G_{\text{BaSi}_2}(P) + (30 \times 1)G_{\text{cd-Si}}(P)}{54}, \quad (1)$$

where $G_{\text{Ba}_8\text{Si}_{46}}(P)$, $G_{\text{BaSi}_2}(P)$, and $G_{\text{cd-Si}}(P)$ are Gibbs free energies per atom at a pressure, P , for Ba₈Si₄₆, BaSi₂, and cd-Si, respectively. $G(P)$ can be evaluated using the simple Legendre transformation of associated equation of state. Using Eq. (1), we can judge relative thermodynamic stability between Ba₈Si₄₆ and the coexisting phase of BaSi₂ and cd-Si for the chemical composition of Ba:Si=8:46. In Fig. 3(c), we

TABLE III. Calculated atomic volume (V_0 , $\text{\AA}^3/\text{atom}$), total energy (E_{total} , eV/atom), cohesive energy (E_{coh} , eV/atom), bulk modulus (B_0 , GPa), and its pressure derivative (B') for bcc-Ba, cd-Si, BaSi, BaSi₂, Si₄₆, Ba₂Si₄₆, Ba₆Si₄₆, and Ba₈Si₄₆. Since the bulk modulus deduced using the Murnaghan's equation of state is strongly sensitive to its pressure derivative (B'), bulk moduli assuming $B' = 3.7$ of Si₄₆ are also listed in parentheses for Ba _{x} Si₄₆ ($x = 2, 6, \text{ and } 8$).

	bcc-Ba	cd-Si	BaSi	BaSi ₂	Si ₄₆	Ba ₂ Si ₄₆	Ba ₆ Si ₄₆	Ba ₈ Si ₄₆
V_0	53.863	19.471	29.321	26.852	22.190	21.501	19.918	19.606
E_{total}	-701.859	-108.242	-405.537	-306.508	-108.153	-132.950	-176.879	-196.370
E_{coh}	1.90 ^a	4.63 ^a	3.75	4.11	4.54	4.49	4.46	4.41
B_0	10	95	44	53	83	84 (85)	87 (89)	85 (88)
B'	2.4	3.7	3.1	3.7	3.7	3.8	3.9	4.0

^aReference 40.

show the variation of relative Gibbs free energy (relative enthalpy) of Ba₈Si₄₆ to the coexisting phase of cd-Si and BaSi₂ in the case of atomic composition of Ba:Si=8:46 with pressure. Though these two phases are almost degenerate in energetics under relatively low pressures, the energetic degeneracy is noticeably broken under higher pressures. That is, the driving force for the conversion to Ba₈Si₄₆ from the mixture of BaSi₂ and cd-Si becomes larger with an increase of pressure. We have experimentally reported that the arc-melted prepressured sample is a mixture of BaSi₂ and cd-Si.⁷ In addition, the conversion to Ba₈Si₄₆ from this mixture has been found to be not completed, if the applied pressure is lower than 2 GPa.⁷ Therefore, the enhancement of the driving force for the conversion to Ba₈Si₄₆ is assumed to play an important role in the success of synthesizing this Ba-doped clathrate compound under high pressures. Using the equilibrium volumes listed in Table III, the atomic volume of the mixture of BaSi₂ and cd-Si in the case of Ba:Si=8:46 is calculated by 22.751 $\text{\AA}^3/\text{atom}$. In contrast, the atomic volume of Ba₈Si₄₆ is 19.606 $\text{\AA}^3/\text{atom}$, which is about 14% smaller than the reactant mixture. Therefore, high-pressure conditions should favor the formation of Ba₈Si₄₆, though the clathrate structure has appeared to be loosely packed compared with cd-Si. A point to notice here is that the structural transition from type-II clathrates (Si₁₃₆) to β -tin phase has been experimentally observed on pressurization above 8 GPa, as mentioned above.^{43,44} While transition properties of type-I clathrate compounds under high pressures have not been experimentally reported, such transitions will affect the form of the high pressure phase relations in these Ba-doped Si₄₆ clathrate compounds. More experiments are needed to understand this point more clearly.

Recently, Fukuoka *et al.*⁴⁵ have successfully synthesized a new silicon clathrate compound of Ba₂₄Si₁₀₀ from a mixture of BaSi₂ and cd-Si utilizing high pressures, in which they have also found that the synthesis using a pressure higher than 3 GPa at 800°C gives a mixture of Ba₈Si₄₆ and cd-Si. While the equation of state of this new clathrate compound, Ba₂₄Si₁₀₀, has not been calculated, high pressure synthesis of silicon compounds will be a promising method for developing new silicon-based materials.

B. Experimental structural properties

The Rietveld refinement pattern of Ba₈Si₄₆ is shown in Fig. 4 along with the experimental pattern. The crystallo-

graphic data of this compound determined by the Rietveld refinement are summarized in Table IV. The clathrate compound of Ba₈Si₄₆ is isomorphous with Na₈Si₄₆ ($a = 10.19 \text{ \AA}$).¹ All of the peaks of the diffraction pattern can be indexed on the basis of a cubic unit cell ($Pm\bar{3}n$, No. 223) of $a = 10.3279 \text{ \AA}$. The lattice constant and the atomic coordinates given in this table are in good agreement with those in the previous work.⁷

Ba₈Si₄₆ is composed of two types of silicon cages of Si(20) and Si(24) linked by sharing a pentagonal face with each other. Ba atoms in the ideal Ba₈Si₄₆ should occupy endohedrally in all of these silicon cages. We have, however, found the missing 12% of some endohedral Ba atoms in the small cage of Si(20) in the present analysis (see Table IV), while the big cages of Si(24) are found to be completely occupied by Ba elements. The observed missing of the Ba atoms in the small unit of Si(20) is presumably due to the site preference of Ba atoms between the $d(6)$ and $a(2)$ sites, as theoretically mentioned in the previous section. In the NMR study of metal-doped Si₄₆ clathrate compounds such as Na _{x} Ba _{y} Si₄₆ and Na₈Si₄₆, Shimizu *et al.*⁴⁶ and Ramachandran *et al.*⁴⁷ have observed three distinct ²⁹Si signals with a different Knight shift. In these two experimental reports, the main three peaks of ²⁹Si NMR spectra of the clathrate compounds can be assigned by using the integrated intensities, which correspond to the ideal stoichiometry of three in-

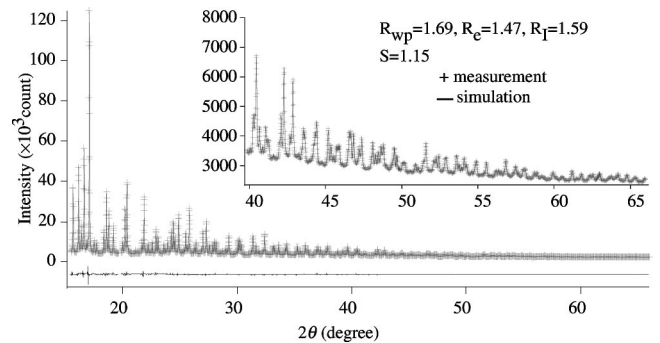


FIG. 4. Rietveld refinement patterns for Ba₈Si₄₆. X-ray-diffraction patterns between 40° and 65° are magnified in the inset. Observed, simulation, and difference patterns are indicated by plus marks (+), and solid, and solid bottom lines, respectively. The experiment pattern is in good agreement with the simulated one in all 2θ region.

TABLE IV. Crystallographic data for $\text{Ba}_8\text{Si}_{46}$ obtained by Rietveld refinement. Lattice parameters, occupations, isotropic thermal parameters (B_0), and atomic coordinates are listed. The previous results using the conventional x-ray-diffraction experiment in Ref. 7 are also listed for comparison.

		Present work		Ref. 7	
Symmetry		$Pm\bar{3}n$ (223)		$Pm\bar{3}n$ (223)	
Lattice constant (\AA)		10.3279		10.328(2)	
Site	Occupation	B_0 (\AA^2)	Atomic coordinates	B_0 (\AA^2)	Atomic coordinates
Si: $c(6)$	0.97	0.74	$x=1/4; y=0; z=1/2$	0.26(32)	$x=1/4; y=0; z=1/2$
Si: $i(16)$	0.98	0.66	$x,y,z=0.1852$	0.38(25)	$x,y,z=0.1864(6)$
Si: $k(24)$	1.00	0.80	$x=0; y=0.3066$ $z=0.1215$	0.35(21)	$x=0; y=0.3055(9)$ $z=0.1199(10)$
Ba: $a(2)$	0.88	0.78	$x,y,z=0$	2.05(19)	$x,y,z=0$
Ba: $d(6)$	1.00	1.22	$x=1/4; y=1/2; z=0$	0.71(10)	$x=1/4; y=1/2; z=0$
Reliability factors ^a (%)			Reliability factors ^a (%)		
$R_{\text{WP}}=1.69, R_e=1.47, R_f=1.44, R_I=1.59$			$R_{\text{WP}}=14.88, R_e=6.31, R_f=4.39$		
Goodness of fit: $S(=R_{\text{WP}}/R_e)=1.15$			$S(=R_{\text{WP}}/R_e)=2.36$		

^a R_{WP} : R -weighted pattern, R_e : R expected, R_f : R structure, and R_I : R integrated intensity.

equivalent Si sites $c(6)$, $i(16)$, and $k(24)$. In contrast, Sakamoto *et al.*⁴⁸ have reported that the ratio of the intensities of ^{29}Si NMR spectrum of $\text{Ba}_8\text{Si}_{46}$, which has been synthesized utilizing the same method as the present sample, are different from that of the number of the distinct Si sites. The missing endohedral Ba atoms in the small cage of Si(20) is presumed to affect the electronic states of framework silicons. In addition, the framework Si sites in the clathrate compound with missing Ba atoms in Si(20) cages cannot be classified into the three inequivalent Si sites. Therefore, a cause of the deviation of ^{29}Si NMR spectrum intensities from the ideal stoichiometry of framework sites observed in $\text{Ba}_8\text{Si}_{46}$ may be related to some of the missing endohedral Ba atoms in the small cage of Si(20). However, a final understanding of this point will have to await further work.

The missing of the framework elements in clathrate structures has also been experimentally reported by some researchers.^{9,49} For example, Herrmann *et al.*⁴⁹ have presented experimental evidence for the missing half of the Ge atoms on the $c(6)$ positions connecting the Ge_{20} clusters in the Ba-doped Ge_{46} clathrate. The similar missing of the framework elements has been experimentally reported in the Sn clathrate of $\text{Cs}_8\text{Sn}_{44}$ which has two vacancies per unit cell.⁹ Table IV shows that Si occupancies at the $c(6)$ and $i(16)$ sites are slightly smaller than that at the $k(24)$ site. Since the accuracy of occupancies on the present refinement has been about 0.3% and the goodness of fit S has been small enough, this result may possibly suggest that there is a little site dependence for Si occupancy in the present sample of $\text{Ba}_8\text{Si}_{46}$ and the missing framework elements in $\text{Ba}_8\text{Si}_{46}$ synthesized under high pressures is lower than that in the Ba-doped Ge_{46} (Ref. 49) and Cs-doped Sn_{46} clathrate compounds.⁹ However, the real stoichiometry of these clathrate samples can be strongly dependent on sample preparation routines, and also on the quality of analysis of the x-ray data. Therefore, it is necessary to actually perform the refinements in the same conditions in order to get the absolute

contents and accurate sites for vacancies in the framework of these clathrate structures. More experiments are needed to quantitatively discuss the occupancy properties of framework vacancies among these clathrate compounds

Nolas *et al.* have reported structural properties and thermal conductivity of Ge type-I clathrate compounds, $\text{Sr}_8\text{Ga}_{16}\text{Ge}_{30}$ and $\text{Eu}_8\text{Ga}_{16}\text{Ge}_{30}$, which are potential candidates for thermoelectric applications.¹⁰ The low-thermal conductivity found in these compounds has been attributed to the dynamic ‘‘rattling’’ introduced by the endohedral ‘‘guest’’ atoms inside the polyhedral cages.¹⁰ Therefore, the thermal parameters, or atomic displacement parameters (ADP’s) of endohedral atoms are important aspects of clathrate compounds. We have found the isothermal parameter of Ba [$d(6)$] in the big cage of Si(24) is larger than that of Ba [$a(2)$] in the small Si(20) unit, while the Ba [$a(2)$] has ADP that is almost the same in magnitude to those of the Si framework atoms. Similar qualitative results of ADP’s have also been experimentally reported on in Ge clathrate compounds.^{10,50} Dong *et al.*²³ have calculated adiabatic potentials of endohedral atoms of alkali and alkali-earth elements as a function of their displacements in the cages of Ge type-I clathrate structures. In their calculations, the potential energy curves of these ‘‘guest’’ elements in the large cages have been found to be relatively flat compared with those in the small cages.^{23,26} Using almost the same theoretical technique, Blake *et al.* have also shown that ADP of Sr in the large cage of $\text{Sr}_8\text{Ga}_{16}\text{Ge}_{30}$ is larger than that in the small cage.^{24,25} The property of ADP’s of endohedral Ba atoms in $\text{Ba}_8\text{Si}_{46}$ experimentally confirmed is in reasonable agreement with these theoretical predictions.^{23–26}

IV. CONCLUSIVE REMARKS

We have presented a joint experimental and theoretical study of the stability and structural properties of Ba-doped

silicon type-I clathrates $\text{Ba}_8\text{Si}_{46}$ synthesized under high pressures.⁷ From the total energy calculations of some barium silicides within the LDA, we have discussed the thermodynamic stability of $\text{Ba}_8\text{Si}_{46}$ under high pressures. The enhancement of the driving force for the conversion to $\text{Ba}_8\text{Si}_{46}$ from the reactant mixture of BaSi_2 and cd-Si is assumed to play a key role in the success of synthesizing this Ba-doped clathrate compound under high pressures. In addition, we have performed a synchrotron x-ray-diffraction experiment of the $\text{Ba}_8\text{Si}_{46}$ prepared under high pressures, using the BL02B2 powder-diffraction beam line at the SPring8 (Hyogo, Japan). Some of the missing endohedral Ba elements in the small cage of Si(20) have been observed by x-ray crystallography, while the big cages of Si(24) are found to be completely occupied by Ba elements. The present LDA calculation for stabilization energies of Ba atoms in endohedral sites suggests that this is presumably due to energetical site preference of Ba atoms between $d(6)$ and $a(2)$ sites. The isothermal parameter of Ba in the big cage of Si(24) has been found to be larger than that in the small

Si(20) unit, which is consistent with some theoretical predictions in earlier works.

ACKNOWLEDGMENTS

This study was partly supported by CREST, Japan Science and Technology Corporation (JST). The synchrotron radiation experiments were performed at the SPring8 (BL02B2) with the approval of the Japanese Synchrotron Radiation Research Institute (JASRI) (Proposal NO. 2000A0047-ND-np). The authors thank K. Kato (Nagoya university, Japan) for his useful technical advice about x-ray-diffraction experiments at the SPring8. We would like to thank Professor T. Motooka (Kyushu University, Japan), Dr. K. Kamei, and S. Shibagaki (Sumitomo Metal Industries, Ltd.) for helpful discussions. One of the authors (K.M.) would like to thank Dr. G. S. Nolas (Marlow Industries, Inc.) for very fruitful discussions on thermoelectrics in clathrate systems. The authors' gratitude also goes to Dr. S. Kobayashi and Dr. T. Sakai (Sumitomo Metal Industries, Ltd.) for their encouragement with this research.

*Present address: Japan Synchrotron Radiation Research Institute (JASRI), 1-1-1, Kouto, Mikazuki-cho, Sayo-gun, Hyogo 679-5198, Japan.

[†]Author to whom correspondence should be addressed. Electronic address: mori@kiso.amaken.sumitomometals.co.jp (mori@kiso.amaken.sumikin.co.jp).

[‡]Present address: Optoelectronics Technical Div. 1, Toyota-Gosei Co., Ltd., 710 Origuchi, Shimomiyase, Heiwa-cho, Nakashima-gun, Aichi 490-1312, Japan.

¹J. Kasper, P. Hagenmuller, M. Pouchard, and C. Cros, *Science* **150**, 1713 (1965).

²C. Cros, M. Pouchard, and P. Hagenmuller, *J. Solid State Chem.* **2**, 570 (1970).

³K. Tanigaki, O. Zhou, and S. Kuroshima, in *Proceeding of the International Winterschool on Electronic Properties of Novel Materials. Fullerenes and Fullerene Nanostructures* (World Scientific, Singapore, 1996), p. 475.

⁴H. Kawaji, H. Horie, S. Yamanaka, and M. Ishikawa, *Phys. Rev. Lett.* **74**, 1427 (1995).

⁵S. Yamanaka, H. Horie, H. Kawaji, and M. Ishikawa, *Eur. J. Solid State Inorg. Chem.* **32**, 799 (1995).

⁶H. Kawaji, K. Iwai, S. Yamanaka, and M. Ishikawa, *Solid State Commun.* **100**, 393 (1996).

⁷S. Yamanaka, E. Enishi, H. Fukuoka, and M. Yasukawa, *Inorg. Chem.* **39**, 56 (2000).

⁸G. S. Nolas, J. L. Cohn, G. A. Slack, and S. B. Schujman, *Appl. Phys. Lett.* **73**, 178 (1998).

⁹J. L. Cohn, G. S. Nolas, V. Fessatidis, T. H. Metcalf, and G. A. Slack, *Phys. Rev. Lett.* **82**, 779 (1999).

¹⁰G. S. Nolas, T. J. R. Weakley, J. L. Cohn, and R. Sharma, *Phys. Rev. B* **61**, 3845 (2000).

¹¹G. B. Adams and M. O'Keeffe, A. A. Demkov, O. F. Sankey, and Y. M. Huang, *Phys. Rev. B* **49**, 8048 (1994).

¹²S. Saito and A. Oshiyama, *Phys. Rev. B* **51**, 2628 (1995).

¹³A. A. Demkov, W. Windl, and O. F. Sankey, *Phys. Rev. B* **53**, 11 288 (1996).

¹⁴E. Galvani, G. Onida, S. Serra, and G. Benedek, *Phys. Rev. Lett.* **77**, 3573 (1996).

¹⁵M. Menon, E. Richter, and K. R. Subbaswamy, *Phys. Rev. B* **56**, 12 290 (1997).

¹⁶O. F. Sankey, A. A. Demkov, W. Windl, J. H. Fritsch, J. P. Lewis, and M. Fuentes-Cabrera, *Int. J. Quantum Chem.* **69**, 327 (1998).

¹⁷J. Dong, O. F. Sankey, and G. Kern, *Phys. Rev. B* **60**, 950 (1999).

¹⁸J. Dong and O. F. Sankey, *J. Phys.: Condens. Matter* **11**, 6129 (1999).

¹⁹J. Zhao, A. Buldum, J. P. Lu, and C. Y. Fong, *Phys. Rev. B* **60**, 14 177 (1999).

²⁰K. Moriguchi, M. Yonemura, A. Shintani, and S. Yamanaka, *Phys. Rev. B* **61**, 9859 (2000).

²¹K. Moriguchi, S. Munetoh, and A. Shintani, *Phys. Rev. B* **62**, 7138 (2000).

²²J. Gryko, P. F. McMillan, R. F. Marzke, G. K. Ramachandran, D. Patton, S. K. Deb, and O. F. Sankey, *Phys. Rev. B* **62**, R7707 (2000).

²³J. Dong, O. F. Sankey, A. A. Demkov, G. K. Ramachandran, J. Gryko, P. McMillan, and W. Windl, in *Thermoelectric Materials 1998 - The Next Generation Materials for Small-Scale Refrigeration and Power Generation Applications*, edited by T. Tritt, G. Kanatzidis, G. D. Mahan, and H. B. Lyon, Jr. (Materials Research Society, Warrendale, 1999), p. 443.

²⁴N. P. Blake, L. Mollnitz, G. Kresse, and H. Metiu, *J. Chem. Phys.* **111**, 3133 (1999).

²⁵B. B. Iversen, A. E. C. Palmqvist, D. E. Cox, G. S. Nolas, G. D. Stucky, N. P. Blake, and H. Metiu, *J. Solid State Chem.* **149**, 455 (2000).

²⁶J. Dong, O. F. Sankey, G. K. Ramachandran, and P. McMillan, *J. Appl. Phys.* **87**, 7726 (2000).

²⁷M. Imai, T. Hirano, T. Kikegawa, and O. Shimomura, *Phys. Rev. B* **58**, 11 922 (1998).

²⁸D. Vanderbilt, *Phys. Rev. B* **41**, 7892 (1990).

²⁹J. P. Perdew and A. Zunger, *Phys. Rev. B* **23**, 5048 (1981).

³⁰The CASTEP code is available from Molecular Simulations Inc.

- ³¹E. Nishibori, M. Takata, K. Kato, M. Sakata, Y. Kubota, S. Aoyagi, Y. Kuroiwa, M. Yamakata, and N. Ikeda, Nucl. Instrum. Methods Phys. Res. (2001) (to be published).
- ³²F. Izumi, in *The Rietveld Method*, edited by R. A. Young (Oxford University Press, London, 1993), Chap. 13.
- ³³Y. Chen, K.-M. Ho, B. N. Harmon, and C. Stassis, Phys. Rev. B **33**, 3684 (1986).
- ³⁴Y. Chen, K.-M. Ho, and B. N. Harmon, Phys. Rev. B **37**, 283 (1988).
- ³⁵T. Charpentier, G. Zérah, and N. Vast, Phys. Rev. B **54**, 1427 (1996).
- ³⁶A. Currao, J. Curda, and R. Nesper, Z. Anorg. Allg. Chem. **622**, 85 (1996).
- ³⁷K. H. Janzon, H. Schafer, and A. Weiss, Z. Anorg. Allg. Chem. **372**, 87 (1979).
- ³⁸G. K. Ramachandran, J. Dong, J. Diefenbacher, J. Gryko, R. F. Marzke, O. F. Sankey, and P. F. McMillan, J. Solid State Chem. **145**, 716 (1999).
- ³⁹S. L. Fang, L. Grigorian, P. C. Eklund, G. Dresselhaus, M. S. Dresselhaus, H. Kawaji, and S. Yamanaka, Phys. Rev. B **57**, 7686 (1998).
- ⁴⁰W. B. Pearson, Experimental cohesive energies for pure components are available from <http://www.scescape.net/simwoods/elements>.
- ⁴¹M. T. Yin and M. Cohen, Phys. Rev. B **26**, 5668 (1982).
- ⁴²D. Kahn and J. P. Lu, Phys. Rev. B **56**, 13 898 (1997).
- ⁴³A. San-Miguel, P. Kéghélian, X. Blase, P. Mélinon, A. Perez, J.P. Itié, A. Polian, E. Reny, C. Cros, and M. Pouchard, Phys. Rev. Lett. **83**, 5290 (1999).
- ⁴⁴G. K. Ramachandran, P. F. McMillan, S. K. Deb, M. Somayazulu, J. Gryko, J. Dong, and O. F. Sankey, J. Phys.: Condens. Matter **12**, 4013 (2000).
- ⁴⁵H. Fukuoka, K. Ueno, and S. Yamanaka, J. Organomet. Chem. **611**, 543 (2000).
- ⁴⁶F. Shimizu, Y. Maniwa, K. Kume, H. Kawaji, S. Yamanaka, and M. Ishikawa, Phys. Rev. B **54**, 13 242 (1996).
- ⁴⁷G. K. Ramachandran, P. F. McMillan, J. Diefenbacher, J. Gryko, J. Dong, and O. F. Sankey, Phys. Rev. B **60**, 12 294 (1999).
- ⁴⁸H. Sakamoto, H. Tou, H. Ishii, Y. Maniwa, E. A. Reny, and S. Yamanaka, Physica C **341-348**, 2135 (2000).
- ⁴⁹R. F. W. Herrmann, K. Tanigaki, T. Kawaguchi, S. Kuroshima, and O. Zhou, Phys. Rev. B **60**, 13 245 (1999).
- ⁵⁰B. C. Chakoumakos, B. C. Sales, D. G. Mandrus, and G. S. Nolas, J. Alloys Compd. **296**, 80 (2000).